Polymer-Based Optical Waveguide Circuits for Photonic Phased Array Antennas

Suning Tang
Radiant Research, Inc.
3006 Longhorn Blvd., Suite 105
Austin, Texas 78758
Email: suning@radiantr.com

L. Wu, Z. Fu, D. An, Z. Han, and Ray T. Chen
Microelectronics Research Center
University of Texas at Austin
Austin, Texas 78712

ABSTRACT

Photonic phased array antennas (PPA) represent one of the most critical technologies for both national defense and civilian wireless communications. In this paper, we present a novel compact detector-switched polymeric waveguide true-time-delay module, which is a crucial building block for advanced wideband photonic phased array antennas. The photolithographically defined ultra-low-loss polymeric waveguides provide us an attractive solution for achieving ultra long delay time over tens of nsec with ultra fine resolution of less than 1 ps. The two-dimensionally distributed waveguide grating couplers tap the optically encoded microwave signal, propagating along the polymeric channel waveguide, to high-speed photodetectors. These photodetectors can be electrically switched on and off independently for selecting different delay times. The appropriate delay time is equal to the time of flight along the waveguide. We have demonstrated that such optical true-time-delays can be implemented in such a device scheme wit the RF spectrum of 11 GHz to 40 GHz. The optically encoded microwave signals are obtained by using semiconductor-laser-based optical heterodyne technique. Such a monolithic integrated module not only reduces the cost associated with optoelectronic packaging, but also reduces the system payload with an improved reliability.

1. INTRODUCTION

In order to meet advanced airborne requirements, the next generation of phased array antennas should have an increased bandwidth (from 11 GHz to 40 GHz), an improved range and cross-range resolution, capable of providing multiple links simultaneously at reduced cost, weight and power constraints. To satisfy these requirements, optical true-time-delay (TTD) steering techniques must be invoked so that efficient elemental vector summation in the receiving mode or in the transmit mode is independent of frequency, which is crucial for ultra wide band operation for future phased array antennas (PAAs) [1-5].

While a phased-array antenna is an improvement over mechanically scanned antennas, technical challenges remain. So far, a variety of phased array antenna technologies have been developed to include microstrip reflect array antennas with mechanical phasing [6], fiber grating prism [7] and thermo-optically switched silica-based waveguide circuit [8]. These attempts have demonstrated the low-weight potential and some good performance characteristic [9]. The mechanical phased microstrip antennas do not need expensive beam-forming transmission-line networks and/or phase-shifting circuits. The beam steering is provided by the mechanical rotation of each antenna elements. In fiber Bragg grating prism technology, high performance reflection gratings can be easily fabricated in ultra-low-loss optical fibers, but requiring very expensive fast wavelength tunable laser diodes. The thermo-optically-switched silica-based waveguide circuit offers excellent delay time control in a compact structure where the length of waveguide is defined by photolithography. The key building block for this approach is the optical 2x2 switch with high switching speed and very low crosstalk (-40 dB). Optical switches with such high performance have not been demonstrated yet.

Part of the SPIE Conference on Optoelectronic Interconnects VI
San Jose, California • January 1999
SPIE Vol. 3632 • 0277-786X/99/$10.00

There are several severe problems of these existing approaches. For example, they are impossible of providing high-speed beam steering due to the speed limitation of mechanical driving motors, wavelength tunable laser diodes, and/or 2x2 thermo-optic switches. The existing approaches also require very expensive components such as miniaturized motors, wavelength tunable laser diodes, and 2x2 thermo-optic switches, which makes the system impractical for commercial applications. The technique for improving these existing approaches demonstrated so far, in general, add to system complexity, employ very expensive devices, and/or require extremely difficult fabrication processes. A low-cost practical optical true-time-delay line for advanced phased array antennas has not been demonstrated yet.

2. PHOTONIC PHASED ARRAY ANTENNA USING OPTICAL TRUE-TIME DELAY LINES

Present day phased array radar systems comprise a transmitter, receiver, beamformer, signal processor, display, power supplies, and a large number of transmit/receive modules that are at some distance from the central location and in close association with the antenna elements making up the array. For airborne applications, the active electronic device of such radar systems are solid state devices configured as discrete devices on printed circuit boards, integrated circuits on silicon substrate, hybrid integrated circuits, and monolithic microwave integrated circuits, which should be small, light weight, and miniaturized. The optical true-time-delay technology is crucial in advanced airborne phased array radar systems because they are of low loss, immune to electromagnetic pulse and are physically small in size, and light in weight.

The realization of practical, optically controlled phased antenna arrays is currently hampered by the extreme complexity required in efficiently transmitting several hundred signals and microwave delays from the input control to the antenna array of the system. These difficulties are compounded by the demands of advanced phased array systems, including extremely high bandwidth broadcast frequencies (ranging from 11 GHz to 40 GHz), non-mechanical beam forming based on true-time-delay technique, and generating multiple beams at different RF frequencies.

As illustrated in Fig. 1, for a linear array radiating elements with individual phase control, the far field pattern along the direction of can be expressed as [10]

$$E(\Phi,t) = \sum_{n=0}^{N} A_n \exp(i\omega_m t)\exp[\,i(\psi_n + nk_m \Lambda \sin\Phi)] \quad , \qquad (1)$$

where A_n is pattern of the individual element, ω_m is the microwave frequency, $k_m = \omega_m / c$ is the wave vector, ψ_n is the phase shift, Λ is the distance between radiating elements and Φ is the direction angle of array beam relative to array normal. The dependence of the array factor on the relative phase shows that the orientation of the maximum radiation can be controlled by the phase excitation between the array elements. Therefore, by varying the progressive phase excitation, the beam can be oriented in any direction to give a scanning array. For the scanning to be continuous, phase shifters are used to continuously vary the progressive phase. For example, to point the beam at an angle Φ_0, ψ_n is set to the following value,

$$\psi_n = -nk_m \Lambda \sin\Phi_0 . \qquad (2)$$

Differentiating Equation (2), we have

$$\Delta\Phi = -\tan\Phi_0 \left(\frac{\Delta\omega_m}{\omega_m}\right) \qquad \text{(rad)}, \qquad (3)$$

It is clear that for a fixed set of ψ_n's, if the microwave frequency is changed by an amount $\Delta\omega_m$, the radiated beam will drift by an amount $\Delta\Phi_0$. This effect increases dramatically as Φ_0 increases. This phenomenon is the so-called "beam squint", which leads to an undesirable drop of the antenna gain in the Φ_0 direction.

In order to obtain the ultrawide bandwidth from 11 GHz to 40 GHz, it is necessary to implement optical true-time-delay steering technique such that the far field pattern is independent of the microwave frequency [2]. In the optical true-time-delay approach, the path difference between two radiators is compensated by lengthening the microwave feed to the radiating element with a shorter path to the microwave phase-front. Specifically, the microwave exciting the (n+1)th antenna element is made to propagate through an additional delay line of length $D_n = nL(\Phi_0)$. The length of this delay line is designed to provide a time delay

$$t_n(\Phi_0) = (n\Lambda \sin\Phi_0) / c \qquad (4)$$

for the (n+1)th delay element. For all frequencies ω_m, ψ_n is given by

$$\psi_n = -\omega_m t_n(\Phi_0). \qquad (5)$$

With such a delay set-up, when the phase term $nk_m\Lambda\sin\Phi$ inside Eq. (1) is changed due to frequency "hopping", the phase term ψ_n will change accordingly to compensate for the change such that the sum of the two remains unchanged. Thus, constructive interference can be obtained in the direction Φ_0 at all frequencies. In other wards, the elemental vector summation in the receiving mode or in the transmit mode is independent of frequency, which is crucial for ultra wide band operation for future PAAs.

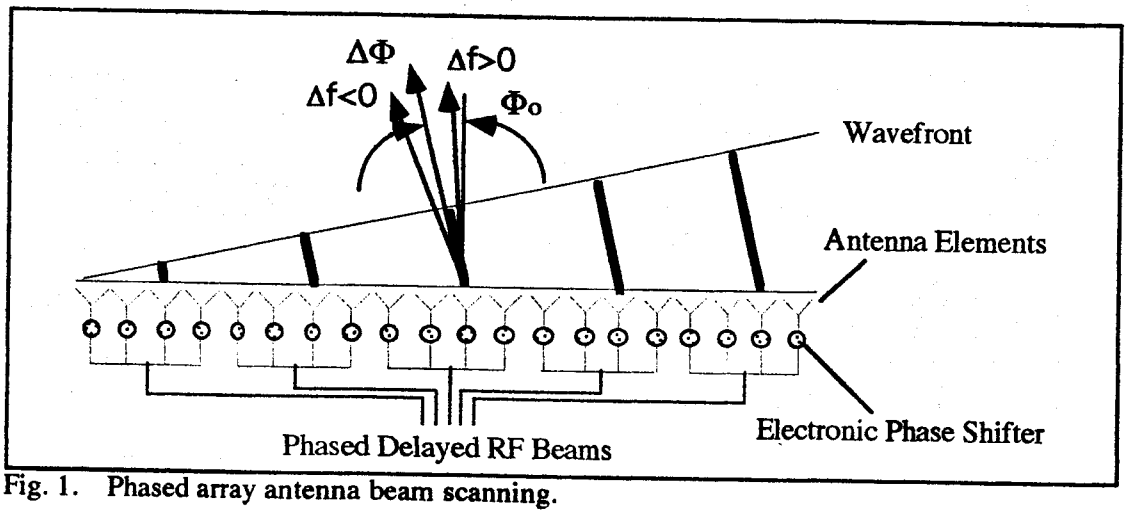

Fig. 1. Phased array antenna beam scanning.

3. ANALYSIS OF A PHOTONIC PHASED ARRAY ANTENNA SYSTEM

Fig. 2 is a typical electrical block diagram of a portion of a novel phased array radar apparatus including an elemental transmit/receive (T/R) module coupled by means of optical paths to the centrally located transmitter and receiver. The RF modulated optical inputs, a single pole single throw (SPST) modulation selection switch and the optical true-time-delay module are provided at the transmitter. The RF modulation of the input optical waves can be provided by using (1) external optical modulator, (2) optical heterodyne technique and (3) directly modulated laser diode. These multiple optical beams are then coupled into the proposed optical true-time-delay module, leading to each T/R module.

The T/R module operates with the antenna elements of the array. In general, one T/R module is required for each antenna element. As the name "T/R module" implies, in transmit periods the T/R module drives the antenna elements with the optical true time delays for maintaining the phase accuracy between antenna elements necessary for beamforming. In receive periods, the T/R module amplifies the signal received by the antenna elements and converts it to an optical format. The optical modulator in the T/R module converts the return signal from the RF format to an optical format suitable for optical RF

transmissions. The optical output of each T/R module is coupled via an optical fiber to an optical detector and preamplifier for connection to one port of a RF summing network of a beamformer. During the receiving period, it is crucial to maintain the phase accuracy between antenna elements necessary for beamforming.

Typically, the laser at the transmitter site is a solid state device, which produces a few miliwatts of signal at a specific wavelength. The laser output is then coupled by an optical divider into a plurality of elemental T/R module [3,10]. The use of optical divider reduces the number of lasers required for a given sized array. The solid state laser of application to present radar system operates at a specific wavelength in the wavelength range of 850 nm, 1300 nm and 1550 nm. The modulation signal can be directly obtained by varying the current through the diode injection with bandwidth from 1 GHz up to 20 GHz. The required RF modulation is often obtained by using an external optical modulator or using optical heterodyne technique [3,10]. The achievable bandwidth is up to 100 GHz. The phase coherence required for beamforming the received signal is maintained by control the phase shifter states and by control of the lengths of the optical path from each elemental T/R module via the detector/amplifier to the RF summing network.

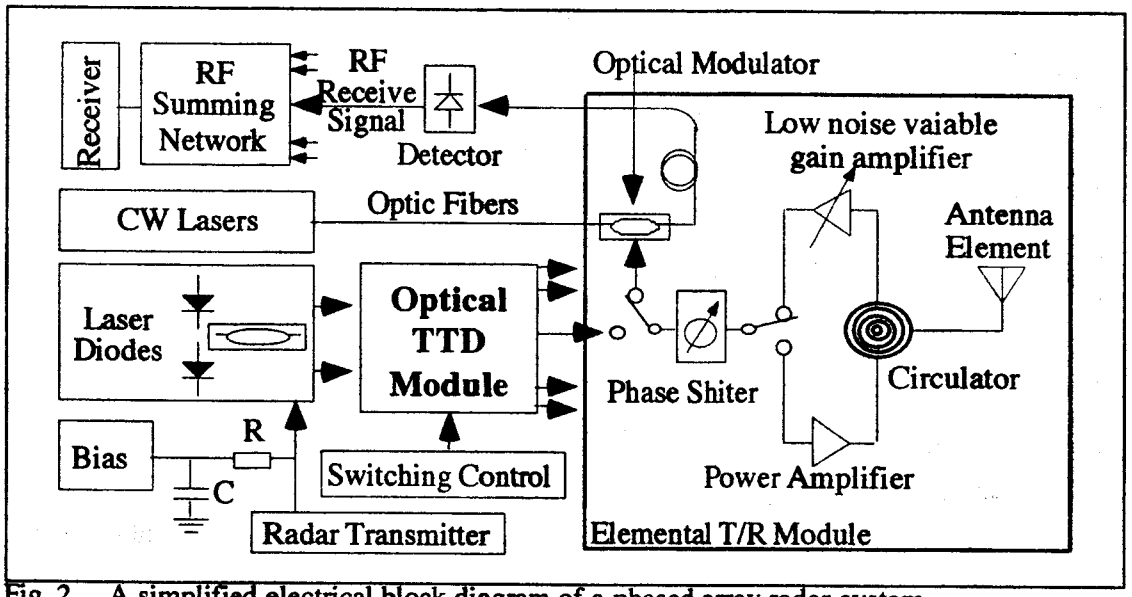

Fig. 2. A simplified electrical block diagram of a phased array radar system.

4. OPTICAL TTD BASED ON PHOTONIC POLYMERIC WAVEGUIDE CIRCUITS

In this paper, we presents a new type of optical true-time-delay lines based on photonic polymeric waveguide circuits in conjunction with electrically-switched high-speed photodetectors shown in Fig. 3, which is capable of providing true-time-delays from 1 ps to 50 ns for wideband multiple communication links in a compact miniaturized scheme. The system uses (1) an innovative ultra long photonic polymeric channel waveguide in conjunction with (2) an array of surface-normal fanout gratings, (3) two laser diodes for generating optical RF carrier based on optical heterodyne technique, and (4) an inexpensive photodetector array. This system eliminates the need for fast wavelength tunable laser diodes, long bulky bundles of fibers and/or expensive optical 2x2 waveguide switches. Unlike any conventional approach where one TTD line can provide only one delay signal at a time, the proposed true-time-delay module is capable of generating all required optical true-time-delay signals simultaneously to all antenna elements. As a result, a large number of true-time-delay combinations can be provided for the phased-array antenna simultaneously by electronic switching the photodetector array fabricated under the polymeric waveguide as shown in Fig. 3. Such a monolithic integration not only reduces the cost associated with optoelectronic packaging, but also reduces the system payload with an improved reliability. A significant reduction of cost, weight, and power consumption is expected.

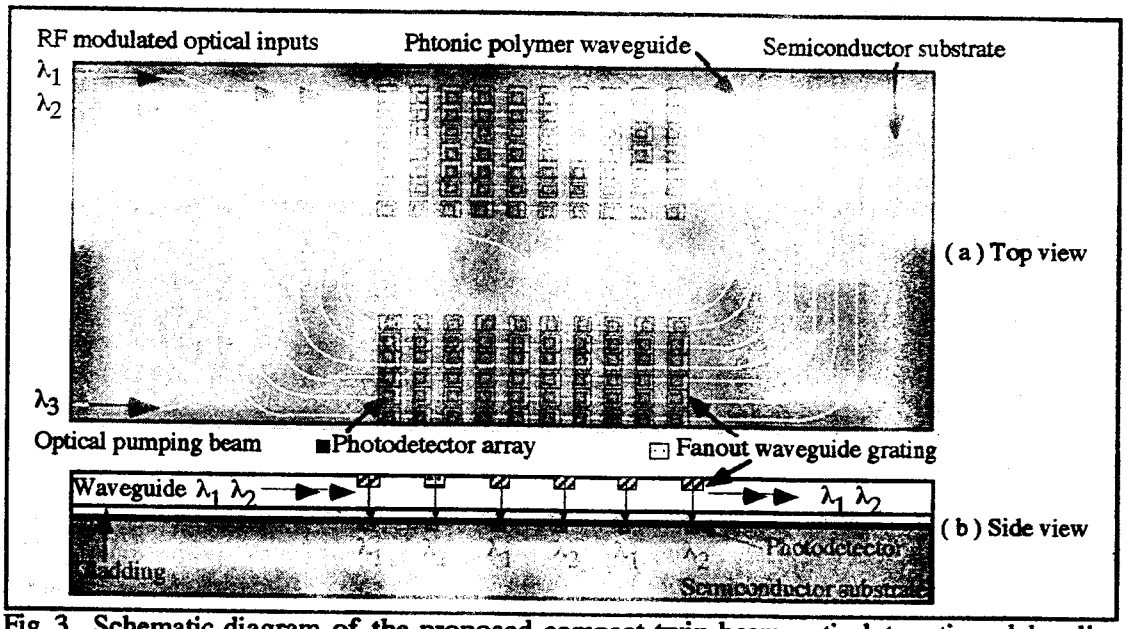

Fig. 3. Schematic diagram of the proposed compact twin-beam optical true-time-delay line based on photonic waveguide. (a) Top view and (b) side view.

Unlike expensive electro-optic switches and wavelength tunable laser diodes, high performance photodetectors are inexpensive and can be cost-effectively fabricated into a large array based on the technologies originally developed for optical imaging and fiber-optic communications. High-speed PIN photodetectors have a typical bias voltage of 3-10 volts with bandwidth up to 100 GHz. The electric diagram of the detector-switched optical true-time-delay module is shown in Fig. 4. Such a hybrid integration of detectors to the optical waveguides eliminates the most difficult optoelectronic-packaging problem associated with the delicate fiber-detector interface and/or fiber-switch interface. It not only reduces the cost associated with optoelectronic packaging, but also reduces the system payload with an improved reliability. A significant reduction of cost, weight, and power consumption is expected.

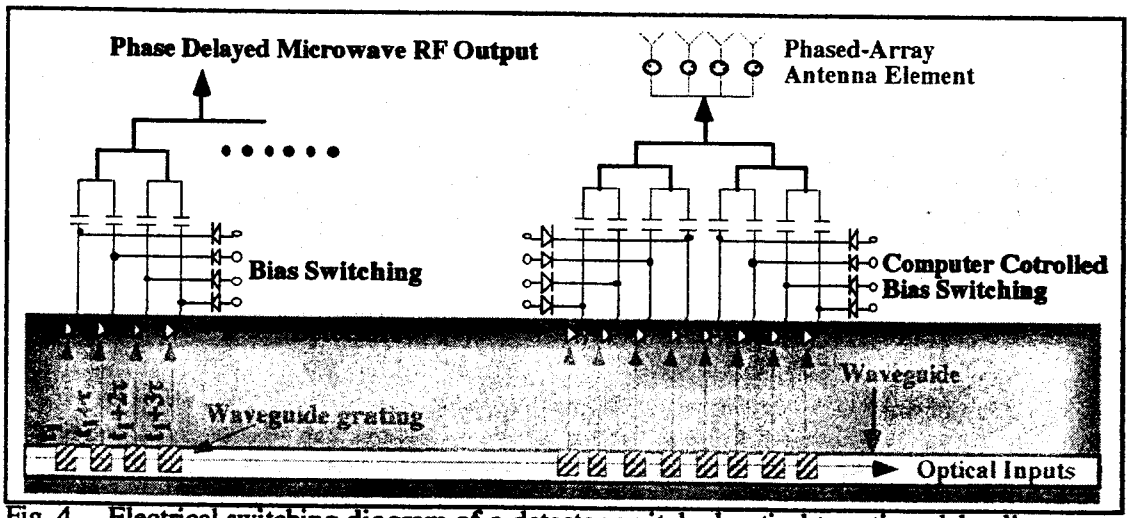

Fig. 4. Electrical switching diagram of a detector-switched optical true-time-delay line.

The unique optical amplification feature of photonic polymers allows us to fabricate a large number of fanout gratings over a ultra long optical channel waveguide [11]. The optical propagation loss and fanout loss is compensated by the optical gain throughout the waveguide delay line. As a result, a large number of time delays can be obtained by using a single laser diode for advanced photonic radar systems that often have 10^3 to 10^5 antenna elements. The optical gain is provided within the photonic polymeric waveguide

doped with rare-earth ions and pumped by a third laser (λ_3) from another end of the waveguide. Note that the details of photonic polymeric waveguide will be published elsewhere. In order to obtain uniform fanout, the optical gain in the waveguide section between two fanout gratings has to be engineered to exactly compensate the sum of the waveguide propagation loss and optical fanout loss. The delay at each detector is equal to the time of flight along the waveguide circuit to the selected waveguide grating coupler. Because the length of waveguides is defined by photolithography, the proposed TTD module can provide a 0.1 ps true-time-delay resolution over a 50 ns dynamic range. The thin film nature of polymers allows us to fabricate the proposed TTD module (made out of waveguide circuits and waveguide gratings) on any substrate of interest, using standard VLSI technologies originally developed for microelectronics industries.

5. MAXIMUM DELAY LENGTH AND MINIMUM DELAY STEP

Another important concern of the phased array antenna is to determine the angular resolution. There is a tradeoff among antenna performance, cost and system weight and size for airborne applications. A large number of antenna elements provide a fine angular resolution, which leads to improved accuracy since the accuracy is directly proportional to beam width. High accuracy is crucial for increasing the communication range and avoiding the information interception by other satellites. However, this also dramatically increases the system weight and cost.

For a PAA with element-to-element spacing of $d = \lambda/2$, where λ is the wavelength of the RF radiation. The maximum possible delay time is equal to [3]

$$T_{imax} = i\lambda \sin\theta_m/2c \qquad i = 1, 2, 3, ..., K \qquad (6)$$

where θ_m is the maximum scan angle, c is the speed of light and K is the number of elements of a PAA. The minimum delay corresponding to the antenna angular resolution θ_R is

$$T_{imin} = i\lambda \sin\theta_R/2c\,. \qquad (7)$$

Eq. (6) and (7) determine the T_{imax} and T_{imin} and the total number R of different delays required for steering the antenna over θ_m with resolution θ_R.

For example, for the designed antenna operating at f =11 GHz (or λ = 27.3 mm), with $\theta_m = 45°$, $\theta_R = 0.7°$, a 6 bits delay line ($R = 2^6 = 64$) is required with T_{max} = 2.06 ns and T_{min} = 35.6 ps, which corresponds to a maximum delay line of $L_{max} = T_{imax}c/n$ = 42 cm, and a minimum delay step of $L_{min} = T_{imin}c/n$ = 7.1 mm, respectively. Here n = 1.5 is the optical refractive index of polymeric waveguide. The antenna element separation is $d = \lambda/2$ = 13.65 mm. The required dimension of the two-dimensional phased array antenna is $S = (dR)^2 = (13.65x64)^2 = 873.6x873.6$ mm^2. As many as 64x64 = 4096 antenna elements may be required. Such a two-dimensional phased array antenna can electronically scan in two-dimension and can cover at least nine satellites at all times in all locations.

6. FABRICATION OF A 10-METER LONG POLYMERIC CHANNEL WAVEGUIDE

In order to realize a high performance phased array antenna, the optical polymeric waveguide may need to be over 10 meters for providing sufficient optical true-time-delay. To fabricate such ultra-long polymeric waveguide circuits, we have developed three waveguide fabrication technologies [12,13,14]:

1. compression-molding technique,
2. VLSI lithography technique, and
3. laser-writing technique.

Our experimental results indicate that high performance polymeric waveguide circuits with waveguide propagation loss less than 0.02 dB/cm can be produced by using laser-writing technique. Compression-molding technique has demonstrated its uniqueness in producing three-dimensional (3D) tapered waveguide

circuits, which is crucial for obtaining efficient optical coupling between the input laser diode and the waveguide circuit. Mass-producible waveguides with excellent repetabitivity have been obtained by using VLSI lithography technique, originally developed for fabricating very large-scale integrated circuits on silicon wafer. Fig. 5 shows the schematic diagrams of three waveguide fabrication technologies developed.

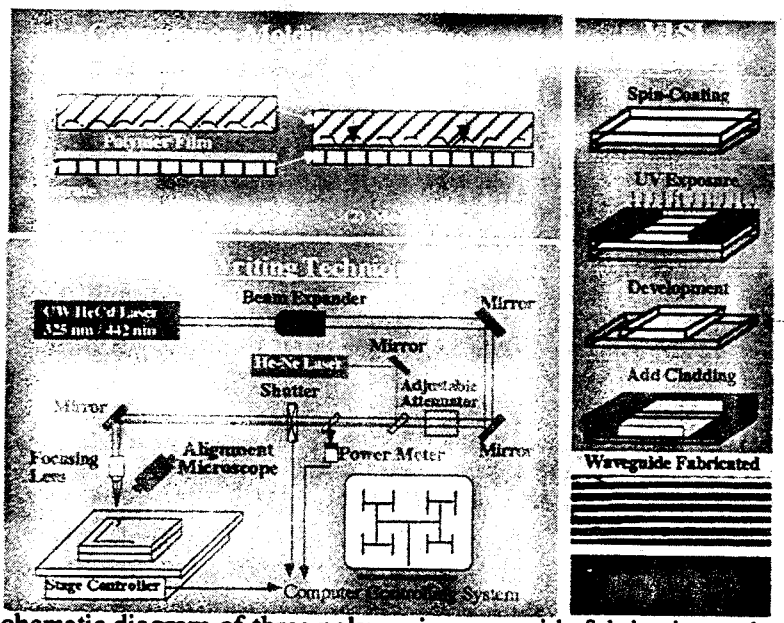

Fig. 5. Schematic diagram of three polymeric waveguide fabrication technologies.

Due to the excellent repeatable results, the ten-meter long polymeric waveguide circuits have been fabricated by using standard VLSI lithography techniques, which is the technology originally developed for microelectronics industries. Since the length of waveguides is defined by photolithography, the waveguide length can be precisely controlled and circled for more than 10 meters with accuracy in the sub-micron range. As a result, the proposed optical true-time-delay module based on polymeric waveguide circuits can provide 0.1 ps true-time-delay resolution over a 50 ns dynamic range. We have successfully fabricated a ten-meter long polymeric waveguide circuit using a VLSI lithography technique. Fig. 6 shows the ten-meter long polymeric waveguide circuit fabricated. The waveguide propagation loss is about 0.02 dB/cm measured at λ = 1064 nm. Ultra-low-loss optical polyimides developed at RRI have been employed for the waveguide fabrication. These polyimides have shown excellent optical transmission characteristics with good thermal and chemical stability over time and temperature. They have been proven to be silicon CMOS process compatible. Detailed information about optical polyimides developed at RRI will be published elsewhere in the near future. It should be noted that same technology has been employed for fabricating waveguide grating couplers as detailed in next section.

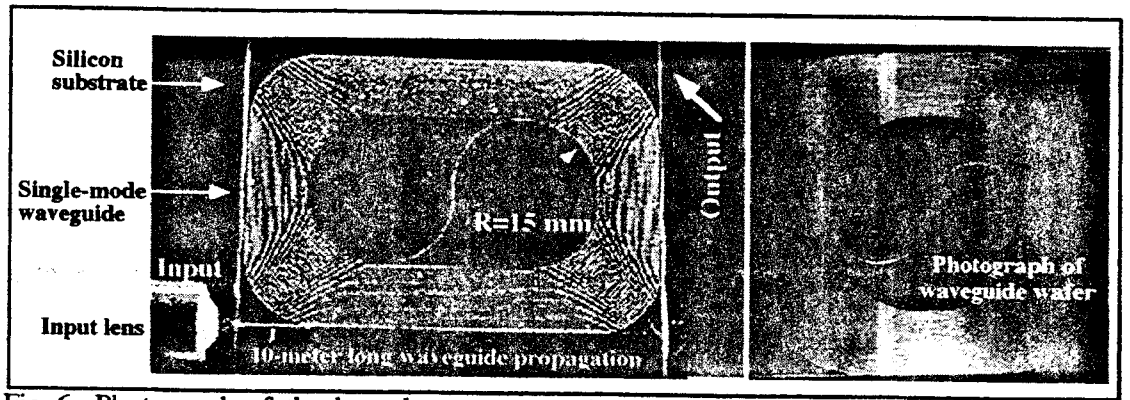

Fig. 6. Photograph of the laser beam propagation through the ten-meter long polymeric channel waveguide.

7. FABRICATION OF TILTED WAVEGUIDE GRATING COUPLERS

The optical waveguide grating couple is an ideal candidate for coupling out the RF modulated optical waves into photodetectors, which propagate through the polymeric waveguide circuit. The unique non-blocking feature of gratings allows us to have a large number of optical fanouts along the waveguide propagation, where each fanout corresponds to a true-time-delay. Since the proposed photonic polymer-based waveguide delay lines are fabricated in a planarized geometry, while the photodetector array employed receives optical signal perpendicular to the substrate surface, surface-normal optical grating couplers are required. In order to provide effective surface-normal coupling, the microstructure of grating coupler should be tilted for creating the required Bragg phase-matching condition just for one output direction. Such surface-normal waveguide grating couplers can be achieved by using tilted surface relief microstructure [13,14] and/or volume holographic dispersive gratings [15,16].

7.1 Calculation of Grating Period and Tilted Angle

It has been found that high quality surface-relief tilted waveguide grating couplers can be fabricated by using standard VLSI fabrication technologies, which are mass-producible at low cost. Conventional grating coupler has an inherent drawback of power loss due to bi-directional diffraction. The most effective technique for overcoming this problem is to employ tilted gratings. In a coupling geometry shown in Fig. 7, we can determine the required grating period Λ as a function of diffraction angle θ_m, diffraction order m, operating wavelength λ, refractive index of waveguide n_1 and refractive index of cladding n_2. The required grating period based on phase-matching condition is

$$\Lambda = \frac{m\lambda n_1}{n_2 \tan\theta_m}[1+\tan^2\theta_m]^{1/2} \qquad (8)$$

If we assume n_1 and n_2 are the refractive index of the superstrate and grating tooth, respectively, the geometrical average of the squared refractive index in the grating region is given by [17]

$$n_g^2 = n_1^2 d + n_2^2(1-d), \qquad (9)$$

where d is the toothwidth-to-period ratio. The optimum tilted angle for first-order Bragg diffraction is given by

$$\theta_{Tilted} = \arccos\frac{\lambda_o}{\Lambda\sqrt{n_g^2 - n_{eff}^2 + \dfrac{2n_{eff}\lambda_o}{\Lambda}}} \qquad (10)$$

where n_{eff} is the effective index of the waveguide structure including the grating, and Λ is the grating period given by Eq. (8).

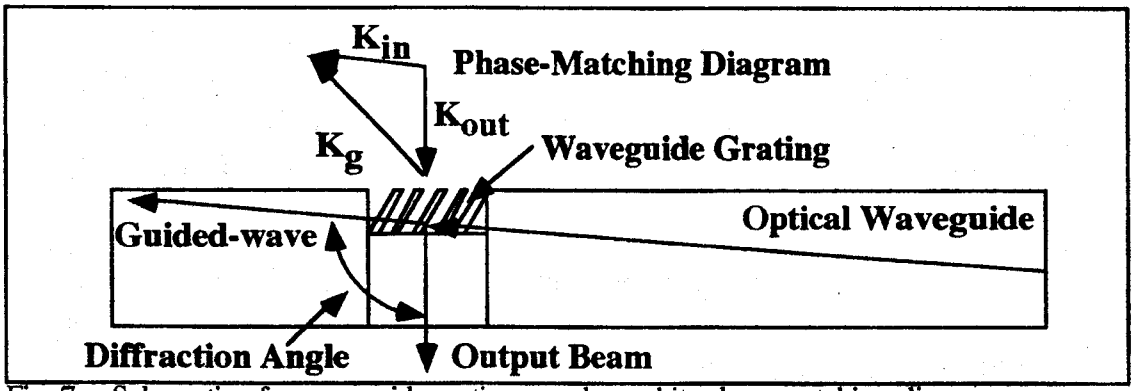

Fig. 7. Schematic of a waveguide grating coupler and its phase-matching diagram.

Based on Eq. (8), $\Lambda = 0.682$ μm is required for the first-order Bragg diffraction when $\lambda = 1.064$ μm, $\theta_m = 90°$, $n_1 = 1.56$ and $n_2 = 1.0$ are assumed. For symmetric grating with the toothwidth-to-period ratio equal to 0.5, the geometrical average of the squared refractive index in the grating region is $n_g = 1.31$ based on Eq. (2). The optimum tilted angle $\theta_{tilted} = 40°$ is obtained by using Eq. (3) when $\Lambda = 0.682$ μm, $\lambda_o = 1.064$ μm, $n_g = 1.31$ are assumed.

7.2 Fabrication of Tilted Waveguide Gratings

Tilted waveguide grating coupler was successfully fabricated by using reactive ion etching (RIE) technique. In this process, the optical channel waveguide was first fabricated using photolithography. For simplicity, glass substrate is selected where waveguide cladding is not required due to the low refractive index of glass. A thin aluminum metal mask is further needed on top of the channel waveguide. A, a 500 Angstroms aluminum layer was coated on top of the waveguide by using electron beam evaporation, followed by a layer of 5206E photoresist with spin speed of 3000 rpm. The grating pattern on photoresist was patterned by a photo mask, which was then transferred to aluminum layer by wet etching, to open a grating-like windows on top of the waveguide. we used a RIE process with a low oxygen pressure of 10 millitorr to transfer the grating pattern on aluminum layer to the polyimide layer. A Faraday cage [30] was used. To form the tilted grating pattern on the polyimide waveguide, the sample inside the cage was placed at a tilted angle of 40 degrees with respect to the incoming oxygen ions. The final step was to remove the aluminum mask by another RIE process. The waveguide tilted grating was successfully fabricated and the scanning electron microscope picture of shown in Fig. 8(c).

Fig. 8 shows (a) the schematic diagram of coupling a laser beam into a polymeric channel waveguide and coupling light out of the waveguide surface-normally using the tilted waveguide grating couplers, (b) the photograph of fabricated device under coupling, and (c) the photograph of tilted waveguide grating. The polymeric channel waveguide is fabricated on an 8 cm long glass substrate, with waveguide thickness of 10 μm and width of 50 μm. The gratings are designed to surface-normally couple the laser beam out of the waveguide with an operating wavelength at 1060 nm. Seven fanout gratings are fabricated on top of the waveguide with 100 mm interaction length and 10 μm separation. In the experiment, a YAG laser with output wavelength of 1060 nm was employed. The seven optical fanouts are clearly observed. The output coupling efficiency is measured at 5%. Coupling efficiency can be well controlled by adjusting the grating depth from 1% up to 8%. As shown in Fig. 8, the non-blocking nature of the waveguide grating allows a large number of fanout along the waveguide propagation. In other wards, a large number of true-time-delay can be generated along the waveguide propagation with the delay time equal to the time of light flight along the waveguide circuit.

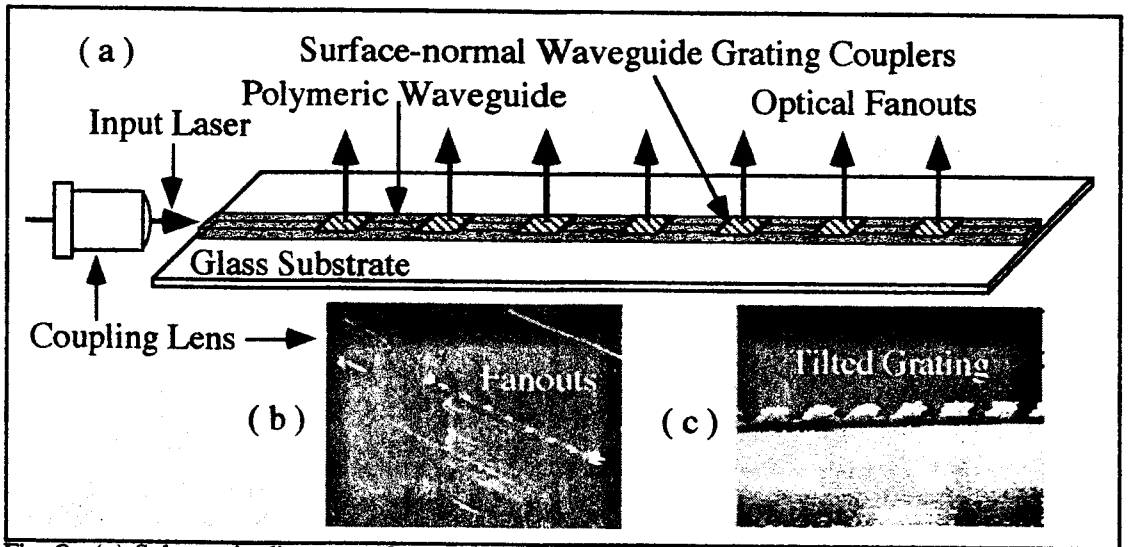

Fig. 8. (a) Schematic diagram of coupling a laser beam into a polymeric channel waveguide and coupling light out of the waveguide surface-normally using the tilted waveguide gratings, (b) photograph of fabricated device under coupling, and (c) photograph of tilted waveguide grating.

8. GENERATION OF 25 GHZ AND 50 GHZ RF SIGNALS

To provide the ultra wideband operation from 11 GHz to 40 GHz, several RF techniques can be employed with different bandwidth tunable capabilities. These include harmonic generation in a Mach-Zehnder modulator [18], heterodyne mixing of two lasers [19], resonance enhanced modulation of a laser diode (LD) [20], and a dual mode DFB laser in mode-locked operation [21]. Direct modulation of laser diode seems straightforward to generate millimeter wave. However, the high insertion loss, high drive voltage, nonlinear response and small modulation depth limit the usefulness of this technique [22].

Compared with direct modulation of a laser diode (LD) or using external modulators, optical heterodyne technique is capable of providing hundreds of GHz base bandwidths while maintaining high modulation depth. We have successfully generates up to 50 GHz RF signals by using two tunable diode lasers oscillating at single longitudinal mode based on optical heterodyne technique. Fig. 9 shows the schematic diagram of the experimental setup. The outputs from these two lasers with slightly different operating wavelengths λ_1 and λ_2 are first coupled into the 10m long polymeric single-mode channel waveguide by using a micro objective lens. This optical output is coupled into a polarization-maintaining fiber and delivered to a high-speed photodetector.

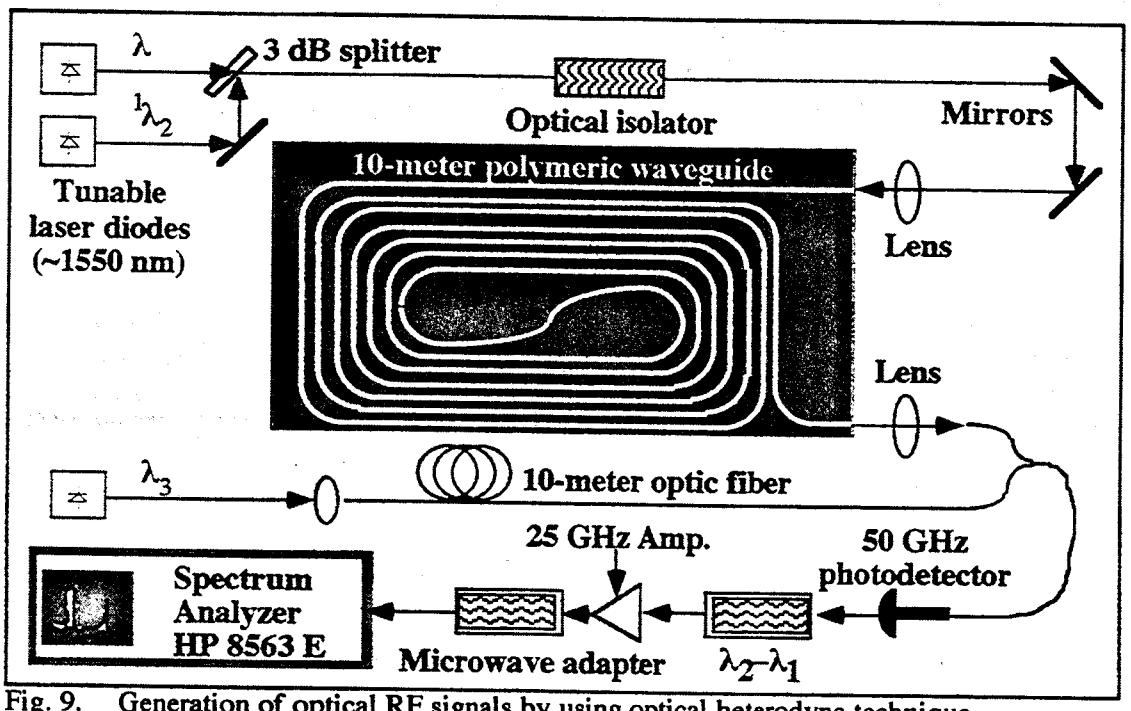

Fig. 9. Generation of optical RF signals by using optical heterodyne technique.

Suppose that the outputs of these two lasers are given by

$$E_1(t) = A_1 \exp(j\omega_1 t), \quad \text{and} \tag{11}$$

$$E_2(t) = A_2 \exp(j\omega_2 t) = A_2 \exp[j(\omega_1 + \Delta\omega)t], \tag{12}$$

where $\Delta\omega$ is the beat frequency. The output of the photodetector is given by [31]

$$i_d(t) = \frac{e\eta}{h\nu}[A_1^2 + A_2^2 + 2F(\Delta\omega)A_1A_2\cos(\Delta\omega)t], \tag{13}$$

where e is the electron charge, η is the quantum efficiency of the detector, $h\upsilon$ is the photon energy, $\omega_1 = 2\pi/\lambda_1$, $\omega_2 = 2\pi/\lambda_2$, and $F(\Delta\omega)$ is the frequency response function of photodetector.

Due to the limitation of the bandwidths of the detector, amplifier, and the spectrum analyzer, optical RF signal above 25 GHz cannot be detected directly. To solve this problem, a third tunable diode laser with wavelength λ_3 between the above two lasers is used to down-convert the high frequency RF signal into two lower frequency signals. For example, a 50 GHz optical beating signal can be converted into two signals at about 25 GHz. In the experiments, the two tunable laser diodes were adjusted to generate a ~50 GHz optical RF beating signal, which was sent directly through the 10 m long optical waveguide delay line fabricated. The optical output from the waveguide end is combined with the output of the third laser and is then sent to 50 GHz photodetector with a 25 GHz microwave amplifier, which is connected to a RF spectrum analyzer. From the measured signals shown in Fig. 10, we get

$$\Delta\omega=\omega1-\omega2=(\omega1-\omega3)+(\omega3-\omega2)=24.85+25.90=50.75\ (\text{GHz}). \qquad (14)$$

Presently, the 50 GHz result is limited only by the frequency responses of the detector, the amplifier, and the spectrum analyzer, but not the optical waveguide true-time-delay module. Since a small tune of the laser wavelength (a few Å) will provide a large beat frequency (tens of GHz), microwave signals as high as several hundred GHz can be readily generated.

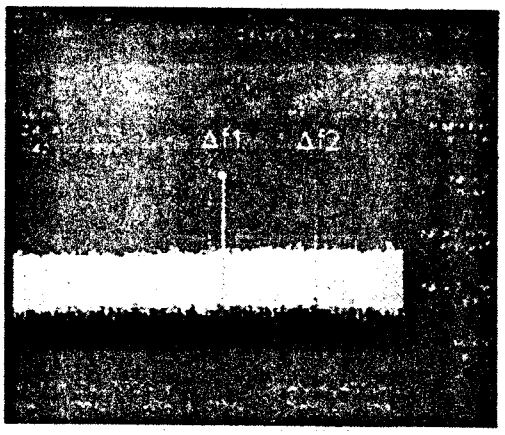

Fig. 10. Demonstration of 50 GHz optical RF signal by the two 25 GHz signals shown on the RF spectrum analyzer.

9. CONCLUDING REMARKS

We have presented a new approach for generating optical true-time-delays by using photonic polymeric waveguide circuits in conjunction with high-speed photodetectors. To realize this concept, we have successfully demonstrated a 10 m long polymeric channel waveguide, with optical propagation loss of ~0.02 dB/cm. Titled waveguide grating couplers are fabricated on top of the channel waveguide to provide surface-normal optical coupling of optically encoded RF signal to photodetectors. These photodetectors, fabricated on the same substrate, can be electrically switched on and/or off independently for selecting different delay times. The photolithographically defined ultra-low-loss polymeric waveguides provide us an attractive solution for achieving ultra long delay time over tens of nsec with ultra fine resolution of less than 1 ps. The appropriate delay time is equal to the time of flight along the waveguide. We have demonstrated that such optical true-time-delays can be implemented in such a device scheme wit the RF spectrum of 11 GHz to 40 GHz. The optically-encoded microwave signals is obtained by using semiconductor-laser-based optical heterodyne technique. Such a monolithic integrated module not only reduces the cost associated with optoelectronic packaging, but also reduces the system payload with an improved reliability.

ACKNOLEDGMENTS

This research is supported by the OSD, AFRL, BMDO, AFOSR, 3M, and Raytheon Systems Co..

10. REFERENCES

1. The fifth annual ARPA symposium on photonic systems for antenna applications, 1995.
2. John E. Midwinter, Photonics in Switching (Academic Press, Boston, 1993).
3. Henry Zmuda, and Edward N. Toughlian, Photonic Aspects of Modern Radar, (Artect House, Inc., Norwood MA 1994), Chapter 13, 17.
4. Zhenhai Fu and Ray Chen, "5-bit substrate guided wave true-time delay module working at 2.4 THz with packing density of 2.5 lines/cm2 for PAA applications", Optical Engineering, vol. 37, pp. 18381841, 1998.
5. L. Xu, R. Taylor and S. R. Forrest, "True time-delay phased-array antenna feed system based on optical heterodyne techniques," IEEE Photon. Technol. Lett., vol. 8, no. 1, pp. 160-162, 1996.
6. J. Huang, "Microstrip refectory antennas with mechanical phasing," NASA Technical Briefs, pp. 54, Dec. 1996.
7. Henry Zmuda, Richard A. Soref, Paul Payson, Steven Johns, and Edward N. Toughlian, "Photonic beamformer for phased array antennas using a fiber grating prism," IEEE Photon. Technol. Lett., vol. 9, no. 2, pp. 241-243, 1997.
8. K. Horikawa, I. Ogawa, T. Kitoh, and Hiroyo, Ogawa, "Photonic integrated beam forming and steering network using switched true-time-delay solica-based waveguide circuits," IEICE Trans. Electron., vol. E97-C, no. 1, pp. 74-79, 1996.
9. A. P. Goutzoulis, and R. P. Gouse, "Comparison of conventional and fiber optic manifolds for a dual band (UHF and S) phased-array antenna," IEEE Trans. on Antennas and propagation, vol. 45, pp. 246-253, 1997.
10. Eli Brookner, Practical Phased-Array antenna systems, Artech house, Boston, 1991.
11. Ray T. Chen, Maggie M. Li, Suning Tang and Dave Gerold, "Nd^{3+}-Doped graded index single-mode polymer waveguide amplifier working at 1.06 and 1.32 mm," Proc. SPIE, Vol. 2042, pp. 462-463, 1993.
12. Suning Tang, et. al., "Compression-molded three-dimensional tapered optical polymeric waveguides for optoelectronic packaging," SPIE, vol. 3005, pp. 202-211, 1997, and IEEE Photon. Technol. Lett., vol. 9, no. 12, pp. 1601-1603, 1997.
13. Suning Tang, Ting Li, F. Li, Michael Dubinovsky, Randy Wickman and Ray T. Chen, "Board-level optical clock signal distribution based on guided-wave optical interconnects in conjunction with waveguide hologram," Proc. SPIE, vol. 2891, pp. 111-117, 1996.
14. Ray T. Chen, Suning Tang, F. Li, L. Wu, M. Dubinovsky, J. Qi, C. Schow, J. Campbell, R. Wickman, "Si CMOS process compatible guided wave optical interconnects for optical clock signal distribution," Invited Paper in IEEE MPPOI'97, vol. 4, pp. 10-24, 1997.
15. Suning Tang, Rob Mayer, Maggie M. Li, and Ray T. Chen, "A novel polymer waveguide wavelength-division-demultiplexer with optical in-plane to surface-normal conversion," IEEE Photon. Technol. Lett., vol. 7, no. 8, pp. 908-910, 1995.
16. Suning Tang and Ray T. Chen, "Intra-Multi-Chip-Module (MCM) optical clock signal distribution," Optics & Phonics News, vol. 5, no. 12, pp. 41-42, December, 1994.
17. Mats Hagberg, Niklas Eriksson, and Anders Larsson, "High efficiency surface emitting lasers using blazed grating outcouplers," Appl. Phys. Lett., vol. 67, no. 25, pp. 3685-3687, 1995.
18. J. J. O'Reilly and P. M. Lane, "Fiber-supported optical generation and delivery of 60 GHz signals", Electron, Lett., 30, 1329, 1994.
19. G. J. Simonis, and K. G. Purchase, "Optical generation, distribution, and control of microwaves using laser heterodyne", IEEE Trans. Microwave Theory Tech., vol. 38, p. 667, 1990.
20. J. B. Georges, M.-H. Kiang, K. Hepell, M. Sayed, and K. Y. Lau, "optical transmission of narrow-band millimeter-wave signals by resonant modulation of monolithic semiconductor lasers", IEEE Photon. Tech. Lett., vol. 6, p. 568, 1994.
21. C. R. Lima, D. Wake, and P. A. Davis, "compact optical millimeter-wave source using a dual-mode semiconductor laser", Electron. Lett., vol. 31, p. 364, 1995.
22. K. Kitayama, "Highly stabilized millimeter-wave generation by using fiber-optic frequency-tunable comb generator", IEEE J. Lightwave Tech., vol. 15, p. 883, 1997.